Journal of Materials Processing Technology 239 (2017) 230–239

Contents lists available at ScienceDirect

Journal of Materials Processing Technology

journal homepage: www.elsevier.com/locate/jmatprotec

In-situ synthesis of titanium aluminides by direct metal deposition

A.N.D. Gasper, S. Catchpole-Smith, A.T. Clare *

EPSRC Centre for Additive Manufacturing and 3D Printing, The University of Nottingham, NG7 2RD, UK

ARTICLE INFO

Article history:
Received 7 December 2015
Received in revised form 25 July 2016
Accepted 26 August 2016
Available online 28 August 2016

Keywords:
Titanium aluminides
Laser
Deposition
Functional grading
Additive manufacturing
AM

ABSTRACT

This study explores the capabilities of methods for in-situ synthesis of titanium aluminides using the Direct Metal Deposition process. This allows for the functional grading of components which will be required for next generation aerospace components. The feasibility of three techniques are explored here; firstly, a new process of powder preparation for Additive Manufacturing, satelliting, in which a larger parent powder is coated with a smaller powder fraction. Here, Al parent particles are satellited with fine TiO_2 to produce an intermetallic matrix composite with Al_2O_3 particulates. The satelliting procedure is shown to increase capability and mixing of in situ synthesis. Secondly, combined wire and single powder feeding is explored through the use of Ti wire and Al powder to create Ti-50Al (at%). Finally, a combination of wire and loose mixed powders is explored to produce the commercially deployed Ti-48Al-2Cr-2Nb (at%) alloy. The simultaneous wire and powder delivery is designed to overcome issues encountered when processing with single powder or wire feedstocks, whilst allowing for on-the-fly changes in elemental composition required for functional grading. Characterisation of the deposits produced, through OM, SEM, and EDX, reveal the influence of key processing parameters and provides a meaningful basis for comparison between the techniques. Results show that it is possible to produce $\alpha_2 + \gamma$ two-phase microstructures consistent with previous studies which have relied upon more expensive and harder to obtain pre-alloyed feedstocks. This represents a move forward in manufacturability for an emergent process type.

© 2016 Published by Elsevier B.V.

1. Introduction

Functionally graded components are key for next generation aerospace parts, where the ability to tailor material properties within the volume of a part for specific function provides great advantages over conventionally manufactured components (Mahamood et al., 2012). These functionally graded components cannot be manufactured through casting and other conventional manufacturing techniques traditionally used for aerospace parts. Additive Manufacturing (AM) technologies such as the Direct Metal Deposition (DMD) process allow these capabilities and design freedoms to be incorporated into a component as it is built up layer by layer. By varying input materials and processing parameters during manufacture, DMD has the potential to grade material both compositionally and microstructurally to vary material properties within the volume of a part. This provides advantages for tailoring different sections of a part for specific functions, a capability not possible through subtractive manufacturing methods which produce bulk material properties. The process also allows for functionally graded hard faces to be applied to components currently in service and the opportunity to not only repair parts but improve damaged parts beyond their previous capabilities. Shishkovsky and Smurov (2012) have demonstrated functional grading of Ti base coatings manufactured via DMD, by incorporating TiN or alumina ceramic (Al_2O_3) for increased hardness, wear resistance and high temperature performance.

Titanium aluminides present an exciting material development with the capability for use in high-temperature and pressure environments that place large demands on mechanical and creep properties of a material (Loria, 2000). They offer a unique combination of low density, good oxidation and ignition resistance, and excellent mechanical properties at high temperature (Appel et al., 2000). With a density of ~3.9 gcm^{-2} titanium aluminides are a potential candidate for a lightweight alternative to nickel-based superalloys (density ~9 gcm^{-2}) currently used for these applications (Dimiduk, 1999). Titanium aluminides are notoriously difficult to process resulting in very high manufacturing costs, in

* Corresponding author at: Room A49, Coates building, University Park, University of Nottingham, NG7 2RD, UK.
E-mail addresses: Alexander.Gasper@nottingham.ac.uk (A.N.D. Gasper), ezxsc3@nottingham.ac.uk (S. Catchpole-Smith), adam.clare@nottingham.ac.uk (A.T. Clare).

http://dx.doi.org/10.1016/j.jmatprotec.2016.08.031
0924-0136/© 2016 Published by Elsevier B.V.

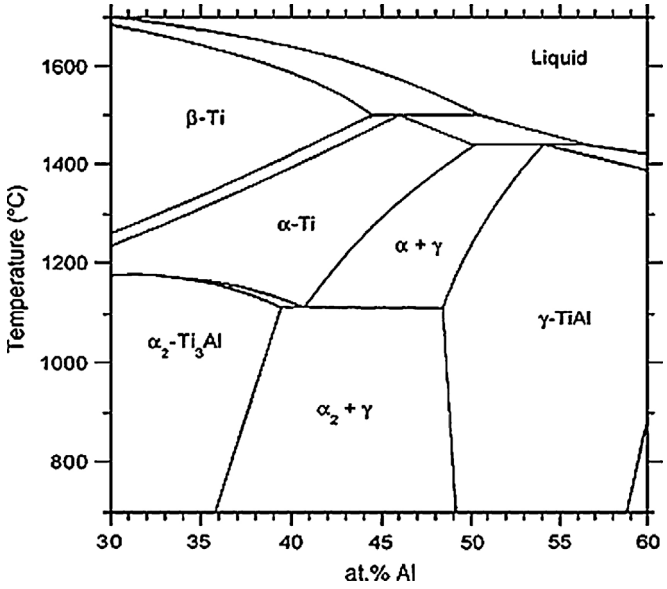

Fig. 1. Modified central portion of the Ti-Al phase diagram taken from Imayev et al. (2007).

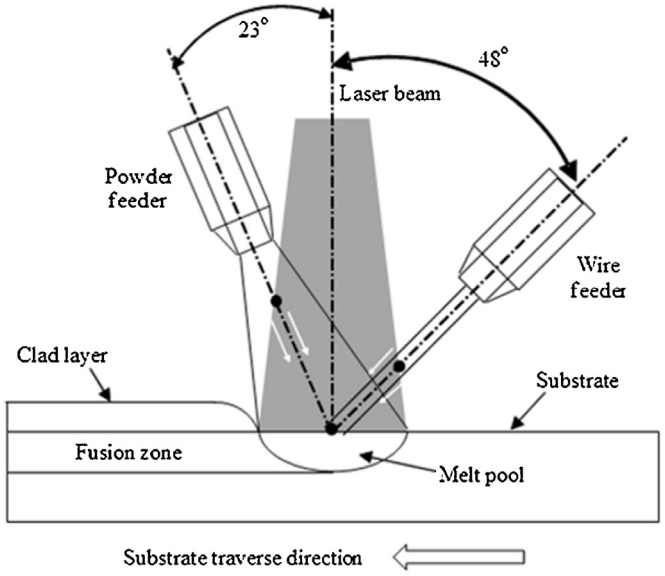

Fig. 2. Schematic of DMD process set up with simultaneous wire and powder feed.

some cases up to 65 times the cost of nickel superalloys (Kothari et al., 2012). Hence there is a need for superior processing routes.

Comprehensive reviews of titanium aluminides are provided by: Loria (2000) reviewed their potential for as structural applications; Appel et al. (2000) reviewed progress in development of titanium aluminides up to the year 2000 related to their mechanical properties and performance; Thomas and Bacos (2011) provided a review on more commercial titanium aluminide alloys and work towards industrial production; and Dimiduk (1999) provided useful comparisons between titanium aluminides and other intermetallic alloys that titanium aluminides have the potential to replace. Dimiduk's comparisons for the mechanical properties required for aerospace applications highlights the potential superior properties of titanium aluminides against other intermetallic alloys. However, Appel et al. (2000) stated that for most of these properties titanium aluminides are currently inferior to nickel-based superalloys, even if the comparisons are made on specific strength alone. This highlights the need for research towards improving these properties and thus enhancing utility. Altering the composition of titanium aluminides has been investigated and micro-additions of elements have been shown to improve properties. Additions of Nb have been shown to increase oxidation and creep resistance and Cr can increase the ductility of titanium aluminides, leading to the development of Ti-48Al-2Cr-2Nb (Kim, 1989), so far the most widely and successfully used titanium aluminide alloy. Many different titanium aluminide alloys have been studied including a wide range of micro-alloying elements all exhibiting different material properties. The advantages of these alloys could be exploited through grading the material within a component from one alloy to another where each would be more appropriate for specific function and service environment (temperatures, pressures, stresses etc.) of particular sections of the component.

The processing of titanium aluminides, presents significant challenge through conventional manufacturing means (Fu et al., 2008). A major challenge is introduced due to the particularly high sensitivity of the mechanical properties to the atomic composition and microstructure of the ordered intermetallic compounds. This is compounded by difficulties in processing without damaging the crystalline structure through mechanical or thermal loading (Lasalmonie, 2006). Ingots produced for forging suffer from coarse grained microstructures with inhomogeneous phase distribution and chemical segregation (Paul et al., 2013). Single (Wang et al., 2000) and often multiple (Liu and Maziasz, 1998) heat treatment procedures are required to achieve final microstructures with acceptable ductility at room temperature whilst retaining high creep strength at elevated temperatures. Titanium aluminides are difficult to machine with their high hardness (up to 454 Hv (Schloffer et al., 2012)) resulting in significant tool wear, poor chip formation, and hence low material removal rates. Therefore net and near-net shape manufacturing processes, such as AM, present themselves as well suited for manufacturing components from this family of materials. Kothari et al. (2012) reviewed the recent advances in processing techniques and a deeper understanding of the material which has been gained, allowing further advancement to be made in this field. This is epitomised in the first commercial uses of titanium aluminide parts used in high performance turbochargers for Formula One and sports cars (Tetsui and Miura, 2002). New processing techniques have facilitated advances towards commercial applications such as with GE and Avio's collaboration with Arcam. This has led to the manufacture of turbine blades with pre-alloyed Ti-48Al-2Cr-2Nb powder using the Electron Beam Melting process, currently used in GE's GENx engines (Thomas and Bacos, 2011). Another powder bed AM process, selective laser melting (SLM), has also been explored for manufacture of TiAl alloys such as beta-solidifying TNM-B1 (Löber et al., 2014) and in-situ TiC particle reinforced TiAl matrix composites. Despite the emergence of titanium aluminide commercial components there is much scope for improving the materials and their manufacture to ensure continued uptake of the material and its establishment as an alternative to nickel superalloys.

This study looks at using the DMD process to produce titanium aluminides through in-situ reactions in order to assess different material preparation methods. Research has been undertaken which explores the use of DMD to produce titanium aluminides but significant shortfalls in the approach have been identified, and the majority of the work to date has related to using pure wire (McElroy et al., 2000) or powder feedstock (Shishkovsky et al., 2012), and in particular pre-alloyed powder feedstocks; Zhang et al. (1998) used pre-alloyed Ti-48Al-2Nb-0.4Ta and Ti-48Al-2Cr-2Nb, and Qu and Wang (2007) pre-alloyed Ti-47Al-2.5V-1Cr, and less investigated methods such as the study by Ma et al. (2014) into in-situ synthesis using elemental Ti and Al wire have been conducted. In this study alternative methods are proposed to improve the manufacturabil-

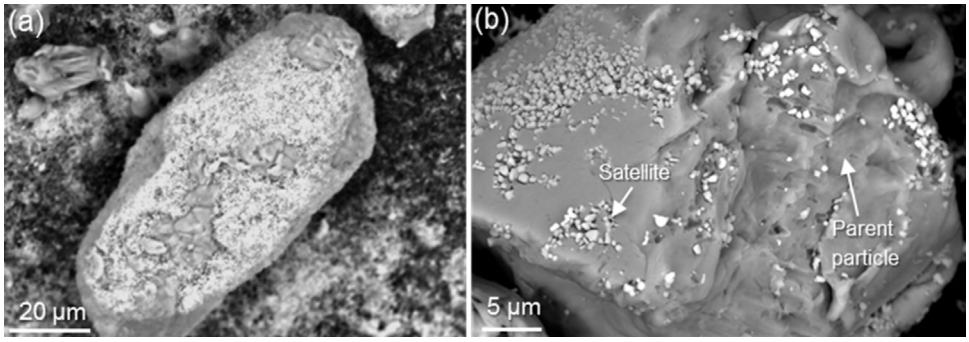

Fig. 3. Micrographs of Al parent particles satellited with fine TiO_2 particles. Concentration of satellites is highly variable, deemed to be a consequence of the irregular and inhomogeneous parent morphology.

ity of these materials. The processes assessed in this study are: the satellite process; a combined wire and single powder feed process; and a combined wire and loose mixed powder feed. The satellite powder process [Patent Application No. 15/022 344] is used to produce an intermetallic matrix composite comprising of multi-phase titanium aluminide matrix with Al_2O_3 particulate reinforcement. This process involves coating a larger parent particle with smaller satellite particles; in this case TiO_2 satellites are adhered to a larger Al parent. Satelliting has the capability to increase the homogeneity and repeatability of in-situ synthesis, whilst also providing cost benefits over using pre-alloyed powders as they can be simply produced with low cost apparatus. The satellited excess material resulting from AM processes can also easily be separated into their constituent powders for reuse or recycling. The key difference in the processing method explored here as compared to that undertaken by Shishkovsky is the use of a titanium precursor, TiO_2, and the use of the laser radiation to initiate reduction reaction to transform this initially into metallic Ti and then intermetallic TiAl. Further, with use of the satelliting technique, a simplified apparatus using a single powder feed nozzle is sufficient to deposit material; previously, a nozzle per feedstock powder would be required for in-situ reaction synthesis. The simultaneous wire and powder processing is used to produce titanium aluminides with varying microstructure and composition for functional grading. Ti wire and Al powder are combined to investigate the production of Ti-50Al. Further investigation includes micro-alloying elements loose mixed with Al powder to produce more advanced titanium aluminides, particularly the Ti-48Al-2Cr-2Nb alloy. This commercially used titanium aluminide has only previously been produced using pre-alloyed powder feedstocks. This study aims to demonstrate the capabilities of in-situ formation for production of these more complex titanium aluminides. The process uses Ti wire and Al powder loose mixed with small quantities of Cr and Nb powders to produce the titanium aluminides. These compositions for the simultaneous wire and powder delivery are designed to produce the two-phase $\alpha_2 + \gamma$ microstructure, see Fig. 1, which has been identified as producing optimum mechanical properties for this system (Thuillard et al., 1988).

The use of combined wire and powder feeds for the DMD process has the potential, according to Syed et al. (Syed et al., 2005) to i) resolve issues arising from using a single source of feedstock including poor capture efficiency and poor laser coupling ii) allowing for compositional and microstructural functional grading reduced material costs and iii) energy usage during processing versus the use of pre-alloyed feedstocks. Compared with multiple wire feedstocks for in-situ processing as explored by Ma et al. (2014) the combined use of a powder feedstock allows for the easy inclusion of different micro-alloying elements. As laid out in the aims of the paper it is to demonstrate a simple and economic method for producing tailored Titanium Aluminide alloys in-situ.

2. Experimental methods

2.1. Equipment

The configuration used was the same for all experimentation; however the wire feeder was not used for the satellite powder

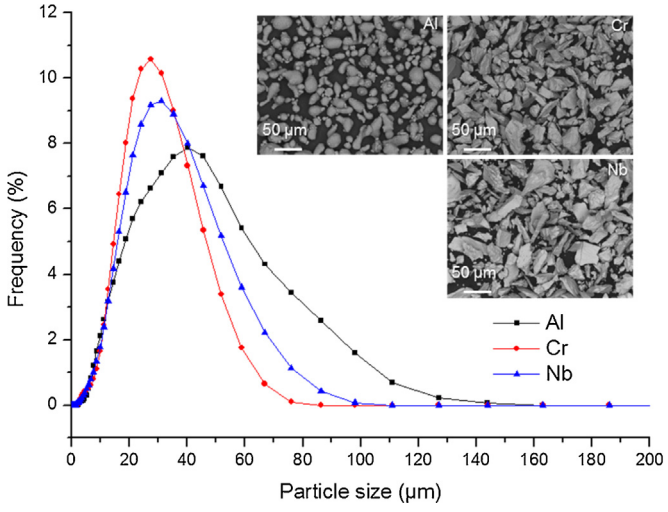

Fig. 4. Particle size distribution of powders using laser diffractometry. The particle sizes relative frequency were collected for 101 bins from 0.01 μm to 3500 μm following the equation y = 0.0088e0.1277x.

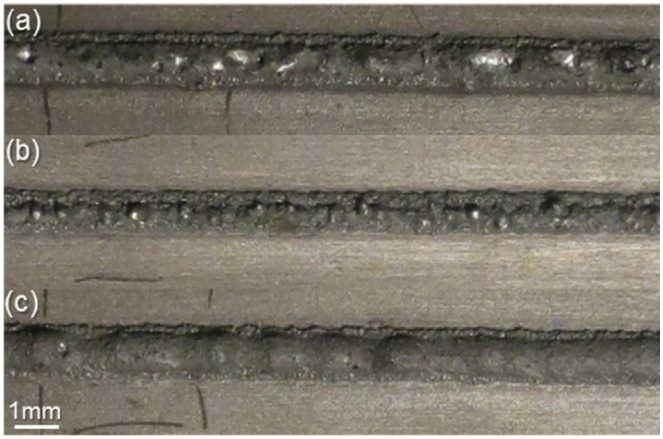

Fig. 5. Tracks produced using satellited powder demonstrating resultant: (a) large pores, (b) balling, and (c) un-melted and partially-melted fused particles.

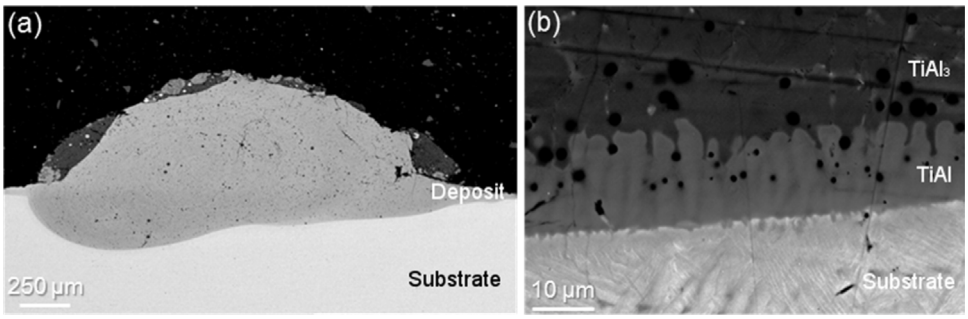

Fig. 6. (a) Satellited powder track produced with 800 W and 4 gmin^{-1}. Excess substrate dilution and asymmetric track bonding caused by high laser power density; (b) substrate-deposit boundary showing formation of additional TiAl phase.

Table 1
Powder compositions used in satellite powder preparation.

	TiO_2	Al
Wt%	20	80
At%	7.78	92.22

Table 2
Powder compositions used in loose mixed powder preparation.

	Al	Cr	Nb
Wt%	81.72	6.56	11.72
At%	92	4	4

Table 3
Processing parameters used for each feedstock technique.

Satellite Powder (SP)	
Parameter	Value
Laser Power (W)	600–800–1000
Traverse Speed (mm min^{-1})	400
Powder Feed Rate (g min^{-1})	2–4–6
Combined Wire and Single Powder (W + SP)	
Parameter	Value
Laser Power (W)	1300–1400–1500–1600
Traverse Speed (mm min^{-1})	400
Powder Feed Rate (g min^{-1})	2–3.2–4.8
Combined Wire and Loose Mixed Powder (W + MP)	
Parameter	Value
Laser Power (W)	1300–1400–1500–1600
Traverse Speed (mm min^{-1})	400
Powder Feed Rate (g min^{-1})	2.4–3.2–4

process. Deposition of the feedstock was performed using a 2 kW Ytterbium-doped, continuous-wave IPG Photonics fibre laser with a wavelength of 1.07 μm. A beam delivery system (125 mm collimating lens and 200 mm focussing lens) and a Precitec YC50 cladding head at a 20 mm defocus provided a 3.1 mm diameter circular beam spot with a Gaussian energy distribution. A Praxair Model 1264 powder feeder back-fed the powdered feedstock through a nozzle at an angle of 23° ± 1 to the beam axis, as depicted in Fig. 2, via an argon carrier gas with a flow rate of 10 l.min^{-1}. A WF200DC wire feeder (Redman Controls and Electronic Ltd) was used to front feed the Ti wire at an angle of 48° ± 1 to the beam axis. The substrate was mounted on a CNC controlled X-Y gantry system. The process is contained within a flexible chamber to create an inert environment. This chamber is purged with argon gas for 15 min prior to deposition and continually flushed at 30 l min^{-1} during deposition, ensuring an environment of <10 ppm of oxygen to minimise oxidation as determined by Mok during experiments using the same apparatus (Mok, 2007).

2.2. Materials

The satelliting preparation technique allows fine particles to be adhered to the outer surface of a larger parent particle. This results in a powder blend with enhanced flow capability compared to a simply loose mixed powder, a key performance factor in the processing of powders for DMD. Further, satelliting prevents separation of the constituent powder fractions, improving the uniformity of chemical composition and consolidation of the deposited alloy. By altering the relative particle ratios between the two powder fractions, multiple alloys with varying chemical composition can be created without the need for expensive pre-alloying. In this study, TiO_2 particles are adhered to Al parent particles. The weight and atomic composition of the powder blend used is depicted in Table 1 and the resultant satellited powders are illustrated in Fig. 3. The Al powder provided by LPW Technology has been characterised as having a particle size range 7–100 μm, with a modal average of 40 μm, the particle size distribution seen in Fig. 4. The fine TiO_2 powder provided by Sigma Aldrich had a maximum particle size of ~1 μm, verified by SEM. An accurate particle size distribution could not be obtained for the TiO_2 powder due to agglomeration preventing adequate flow through the laser particle size apparatus.

The same wire and powder was used for both the combined wire and powder techniques, via the process depicted in Fig. 2. Commercially pure Ti Grade 2 wire with a diameter of 1.2 mm was provided by VBC GROUP, and the Al powder was the same as that used for the satellite powder preparation.

For the loose mixed powder, Cr and Nb powders, provided by Goodfellow Cambridge Ltd., were combined with the Al powder. The loose powders were mixed in the proportions listed in Table 2, with the intention of acquiring Ti-48Al-2Cr-2Nb in the tracks deposited as produced by Cárcel et al. (2014) and Zhang et al. (1998) where more expensive pre-blended powder feedstocks were used. The Cr and Nb had modal averages of 27 μm and 31 μm respectively, their particle size distributions can be seen in Fig. 4. The metallic powders used were all gas atomised and had sufficient flow properties to be compatible with the powder feed system used in this study. Since the DMD method used does not rely upon packing density as in SLM, particle morphology is not deemed to be as critical.

2.3. Processing parameters

The processing parameters for the all the tracks produced are detailed in Table 3, where the experiments are designed to evaluate changes of the processing parameters of powder feed rate (PFR) and laser power (LP) and a single track was produced for each combination of these parameters. The processing parameters were based on the energy densities used by Cárcel et al. (2014) in their study of processing Ti-48Al-2Cr-2Nb, Shishkovsky et al. (2012) processing of functionally graded Ti-Al systems, and preliminary experiments in processing Ti wire and Al powder using DMD.

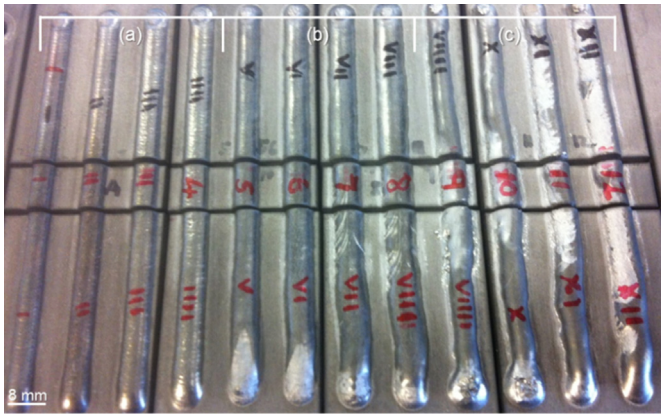

Fig. 7. Morphology of tracks produced with combined wire and single powder delivery. PFR: (a) 2.0 $gmin^{-1}$, (b) 3.2 $gmin^{-1}$, and (c) 4.8 $gmin^{-1}$.

2.4. Deposit characterisation

Cross sections for metallographic analysis were taken from the central section of the 80 mm tracks, as shown in Fig. 7, so as to provide a good representation of the processing. Metallographic specimens were prepared by standard mechanical grinding using 240, 400, 800 and 1200-grit SiC papers and polished using cloths containing 3 μm and 1 μm diamond abrasive. The samples were etched by dabbing over the surface for approximately 5 s with cotton wool soaked in modified Kroll's reagent (2 ml HF, 8 ml HNO_3, and 88 ml H_2O) (Zollinger et al., 2007). The samples produced through wire and powder delivery were also treated with a solution of 70 ml Colloidal Silica and 10 ml H_2O_2 after diamond polishing and preceding etching. This process produced the best results in revealing the microstructure of the deposits.

A Bruker QUANTAX 70 Electron Dispersive X-ray Spectroscopy (EDX) detector was used to analyse the composition of the tracks. For composition results, the SEM beam parameters were optimised to produce a high count per second (CPS) on the EDX detector and measurements were taken from a large area to provide an appropriate approximation of the bulk composition. This was repeated three times in different section of the cross section to provide further representation of the result of the bulk material and to minimise the error of the measurement. The final composition figures are the averages of the three areas and the errors for these averages are provided. For line data acquisition, the scan was run for 10 min to allow sufficient time for any low concentration alloying elements to be detected and for the measurement error to be minimised. It should also be noted that at 15 kV acceleration voltage, electron interaction resulted in an effective spatial resolution of approximately 3 μm below the sample surface and hence some elemental data returned by the EDX equipment may relate to some sub-surface material.

3. Results and discussion

3.1. Track deposits

3.1.1. Satellite powder feedstock

Due to the rapid and highly exothermic reaction between the constituent powders, the deposited tracks have a high surface roughness as a result of un-melted and partially-melted, fused particles as seen in Fig. 5(c), particularly at the periphery of the track. Large pores are present in most tracks, likely caused by the release of oxygen in a gaseous state during reaction synthesis (Fig. 5(a)). At lower LP or when PFR is too high, discontinuous deposition (balling) occurs (Fig. 5(b)).

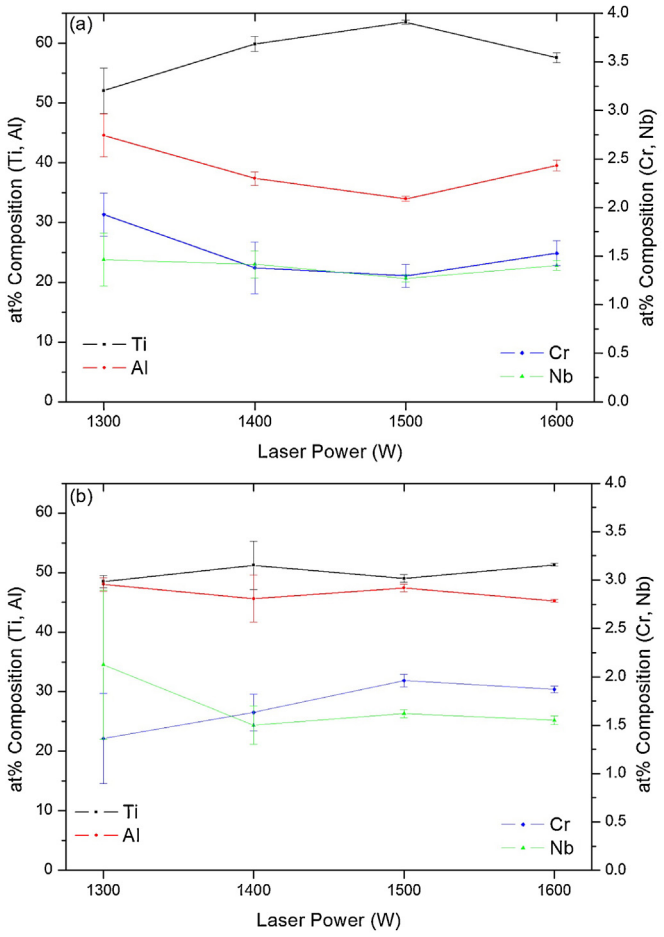

Fig. 8. Composition variations mapped for constituent elements against LP for the wire and mixed powder deposition with PFR (a) 3.2 $gmin^{-1}$ and (b) 4.0 $gmin^{-1}$.

Insufficient laser energy density prevents bonding of the feedstock to the substrate and an inconsistent and widely varying deposit height results. Conversely, some of the tracks exhibit high dilution due to excess laser energy density, characterised by a distinctive shape fusion zone that is deep below the surface of the substrate as seen in Fig. 6. The variation in dilution results in a variation in the mechanical bond strength between the substrate and the deposit. Further, excess dilution significantly alters the chemical composition of the deposit, increasing the probability of the formation of undesirable phases, especially at the substrate-deposit interface. This resulted in cracking at the substrate-deposit interface in some cases. However, little cracking was observed in the bulk of the tracks.

Deposition of Ti-Al intermetallic tracks with an approximate height of 1 mm can be achieved at a laser energy density of 79.5, 106 and 132 Jmm^{-2} by utilising reaction synthesis. This is in comparison with 160–285 Jmm^{-2} and 76 Jmm^{-2} for 0.2–0.3 mm layers required by Cárcel et al. (2014) and Qu and Wang (2007) respectively for the deposition of titanium aluminides without exothermic reaction. Hence, the potential energy savings afforded by the use of reaction synthesis and TiO_2 as a feedstock powder are highlighted. The tracks with the best bonding to the substrate are typically shorter and wider than those with poor bonding. The poor bonding is caused by a lack of feedstock melting and substrate wetting, resulting from insufficient laser energy density, excess PFR, or a combination of these. For component manufacture using DMD, it is suggested that a high LP combined with a reasonably low PFR is required to avoid the onset of internal porosity and un-

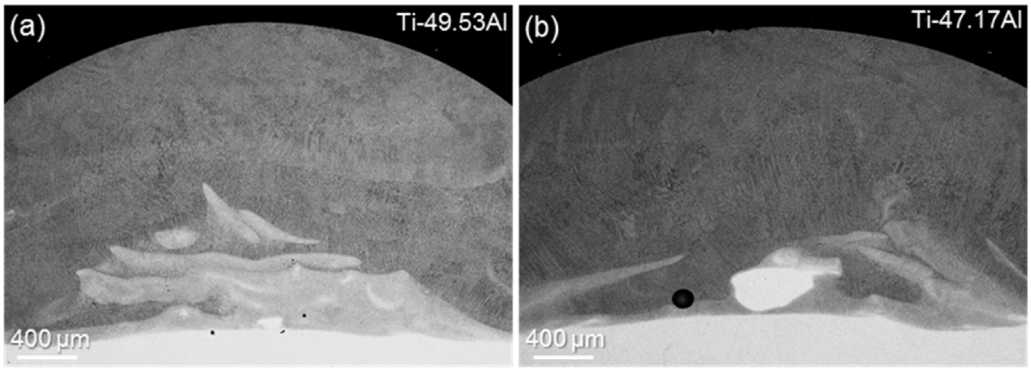

Fig. 9. SEM micrographs of W + SP tracks produced with a 3.2 gmin^{-1} PFR with compositions closest to the desired Ti-50Al at (a) LP 1400 W and (b) LP 1600 W.

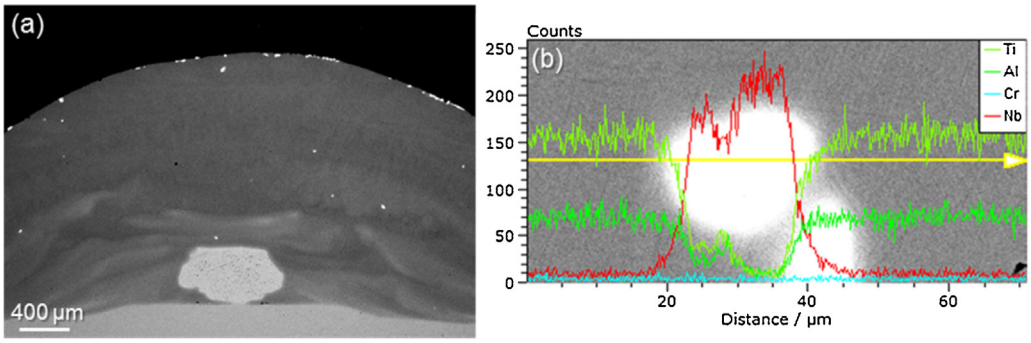

Fig. 10. Track with 3.2 gmin^{-1}, 1400 W and composition Ti-38.21Al-1.35Cr-1.45Nb: (a) SEM image of track showing the central partially-melted Ti wire and dispersed partially-melted Nb particles; (b) Line EDX depicting white particles as Nb.

Table 4
Composition for combined wire and single powder (W + SP) combined wire and loose mixed powder tracks (W + MP) from EDX analysis.

W + SP				
PFR	1300 W	1400 W	1500 W	1600 W
2.0 g min^{-1}	*Ti-26.3Al*	*Ti-27.4Al*	*Ti-28.7Al*	*Ti-28.3Al*
3.2 g min^{-1}	*Ti-48.7Al*	*Ti-49.5Al*	*Ti-50.3Al*	*Ti-47.2Al*
4.8 g min^{-1}	*Ti-35.4Al*	*Ti-59.2Al*	*Ti-53.6Al*	*Ti-52.1Al*
W + MP				
PFR	1300 W	1400 W	1500 W	1600 W
3.2 g min^{-1}	*Ti-42.50Al-1.43Cr-1.87Nb*	*Ti-38.21Al-1.35Cr-1.45Nb*	*Ti-33.46Al-1.26Cr-1.35Nb*	*Ti-38.81Al-1.38Cr-1.60Nb*
4.0 g min^{-1}	*Ti-49.25Al-1.65Cr-2.00Nb*	*Ti-46.17Al-2.5Cr-1.31Nb*	*Ti-48.57Al-1.55Cr-1.90Nb*	*Ti-45.55Al-1.59Cr-1.84Nb*

melted particles (Luo and Acoff, 2004). This also improves the bonding between adjacent tracks with minimal overlap when producing components with multiple layers, important for maximising material deposition rates whilst ensuring full density deposition is achieved.

3.1.2. Simultaneous wire and powder delivery (both single and mixed powder)

Both of the combined wire and powder processes successfully produced fully dense titanium aluminide tracks with good bonding to the substrate for all PFR's. The poor surface quality and porosity witnessed in the tracks produced with the highly exothermic satellited powder blend were not present. The tracks processed with the highest PFR produce more inconsistent deposits with varying width and height as well as surface finish along the track, increased cracking and porosity was also noticed in these tracks. This inconsistency can be seen in Fig. 7, where the lower PFR (a) produces straight, consistent and regular tracks. As the PFR increases, Fig. 7(b) and (c), track morphology and surface quality vary significantly along each track.

3.2. Composition

3.2.1. Combined wire and single powder feedstock (W + SP)

The compositions of the tracks produced were established using EDX. Table 4 shows the compositions of the tracks produced through the simultaneous wire and powder delivery techniques. The results are averaged from spectra taken from multiple points in the cross-section to provide a representative composition for the whole track. Fig. 8 shows a graph of the compositions and the errors for the measurement. With regards to the processing parameters used, no obvious trends are apparent in the composition results and a larger set of data from different processing parameters would be required to establish any.

The tracks processed with a PFR of 3.2 g min^{-1} produced compositions closest to the desired Ti-50Al, however the composition was shown to vary across the cross-section, particularly where the Ti wire had not fully mixed with the rest of the track. Evidence of this lack of mixing can be seen in the SEM micrographs in Fig. 9, the lighter Ti rich sections can be seen in the tracks where the Ti wire has not mixed homogenously with the Al powder. Fig. 9(b), shows the worst of these mixing issues where it is evident that the Ti wire

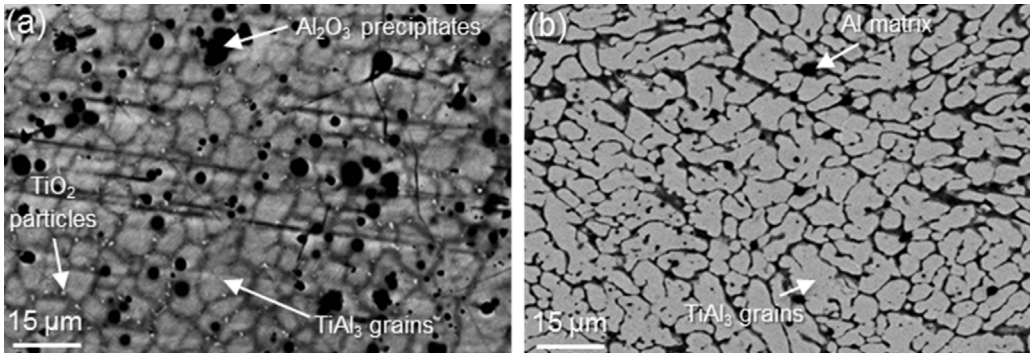

Fig. 11. BSE micrographs of the two distinct deposit microstructures formed: (a) dense equiaxed grains of $TiAl_3$ with Al rich grain boundaries, dispersed Al_2O_3 spherical precipitates and un-reacted TiO2 particles along grain boundaries; (b) early-stage dendritic $TiAl_3$ grains within a high-purity Al matrix.

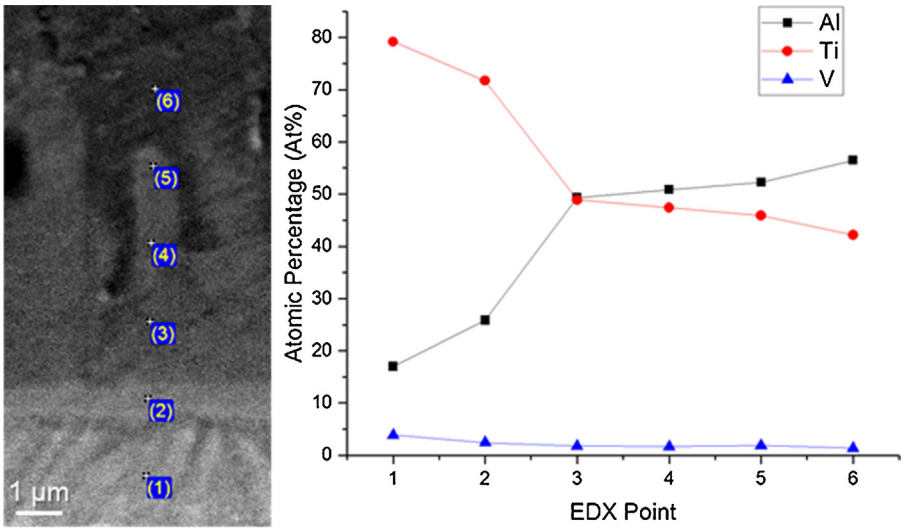

Fig. 12. Line EDX across the substrate-deposit boundary illustrating the formation of TiAl columnar grains due to diffusion across the interface.

has not melted completely. A large area of un-melted Ti wire was encountered in the two tracks with the lowest LP for the 4.8 g min^{-1} PFR but full melting of the wire occurred for the two highest LP.

The tracks produced with the lowest PFR did not experience these mixing and un-melted wire issues. There are two areas where improvements could be made, with the processing parameters and the feedstock input. Energy density incident on the melt pool is the key parameter that should improve the mixing issue, through increasing the amount of flow within the track allowing for greater mixing. An increase in energy density can be achieved through increasing the LP, however this alone cannot ensure that the wire fully melts as shown in Fig. 9(b). Un-melted Ti wire still remains despite processing with the highest LP. Reducing the traverse speed between the substrate and DMD head can also achieve an increase in energy density. This would allow energy to be applied for longer, increasing Marangoni effects that result in improved flow and mixing of the materials. Another possible solution to this mixing issue could be to decrease the overall amount of material being processed. This would allow the materials to absorb more of the energy from the laser ensuring that the Ti wire has sufficient energy to melt and mix with the molten Al, however, deposition rates would be reduced. Whilst the lower PFR, where the mixing issues were less predominant, leads to less material to heat it also leads to less powder obscuring the laser beam and ensuring the energy is applied more directly into the melt pool.

3.2.2. Combined wire and loose mixed powder feedstock (W + MP)

The results from the compositional analysis of the tracks produced through the combined wire and loose mixed powder feedstock show that the desired Ti-48Al-2Cr-2Nb composition is most closely achieved through the 4.0 gmin^{-1} PFR. The tracks show much of the same mixing and melting of the Ti wire issues as displayed in the W + SP tracks. Cr and Nb were detected throughout the tracks, with a variation of ~1.34–2.46 at%, indicating a distribution of the additives within the loose mixed feedstock and the resulting deposit.

One issue discovered in many of these tracks was the occurrence of partially-melted Nb particles as seen in Fig. 10. It is assumed that the presence of only Nb particles and not Cr is due to Nb much higher melting point at 2750 K. Very small amounts were detected within all of the tracks however the majority of the partially-melted Nb particles were located on the edge of the tracks due to the highest heat dissipation being at the periphery.

3.3. Microstructure

3.3.1. Satellite powder feedstock

A variety of microstructures are produced from the in-situ synthesis of the satellite powder using DMD. In all cases, the largest volume fraction consists of either dense equiaxed grains of $TiAl_3$ with Al_2O_3 spherical precipitates or early-stage dendritic $TiAl_3$

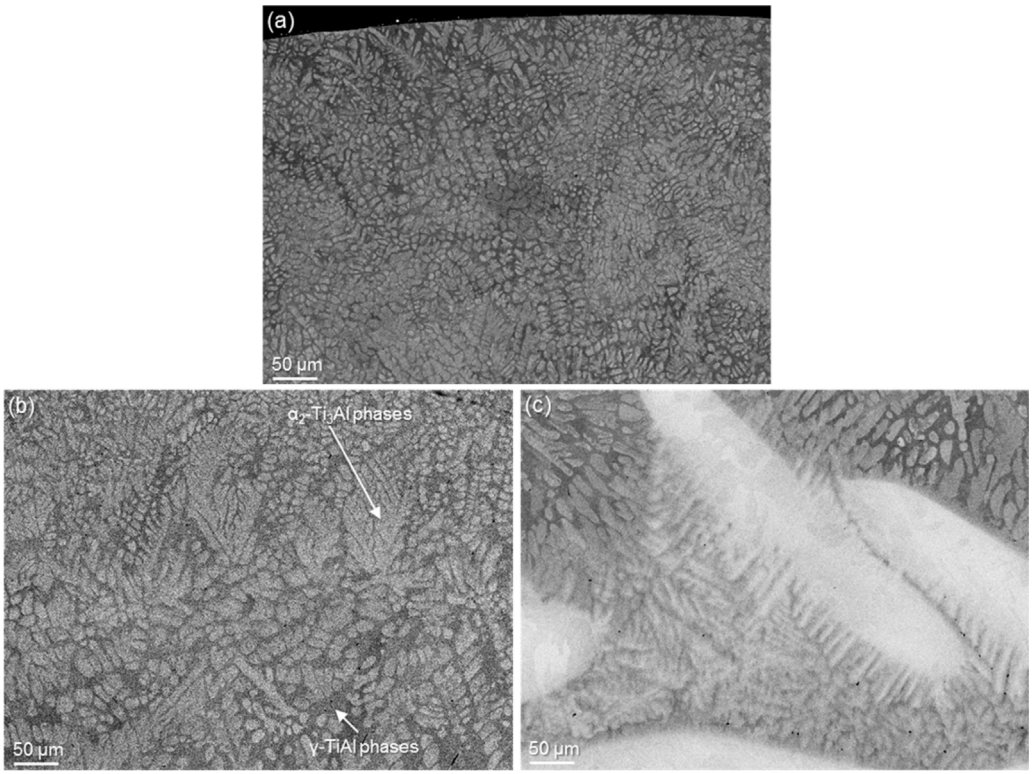

Fig. 13. SEM images of $\alpha_2 + \gamma$ two-phase microstructures produced from W + SP with 1400 W, 3.2 $gmin^{-1}$ and composition Ti-49.63Al: (a) fine equiaxed microstructure due to highest cooling rate; (b) more columnar microstructure with dark TiAl γ-phases and light Ti_3Al α_2-phases; and (c) large Ti rich Ti_3Al α_2 phases due to insufficient melting of the Ti wire.

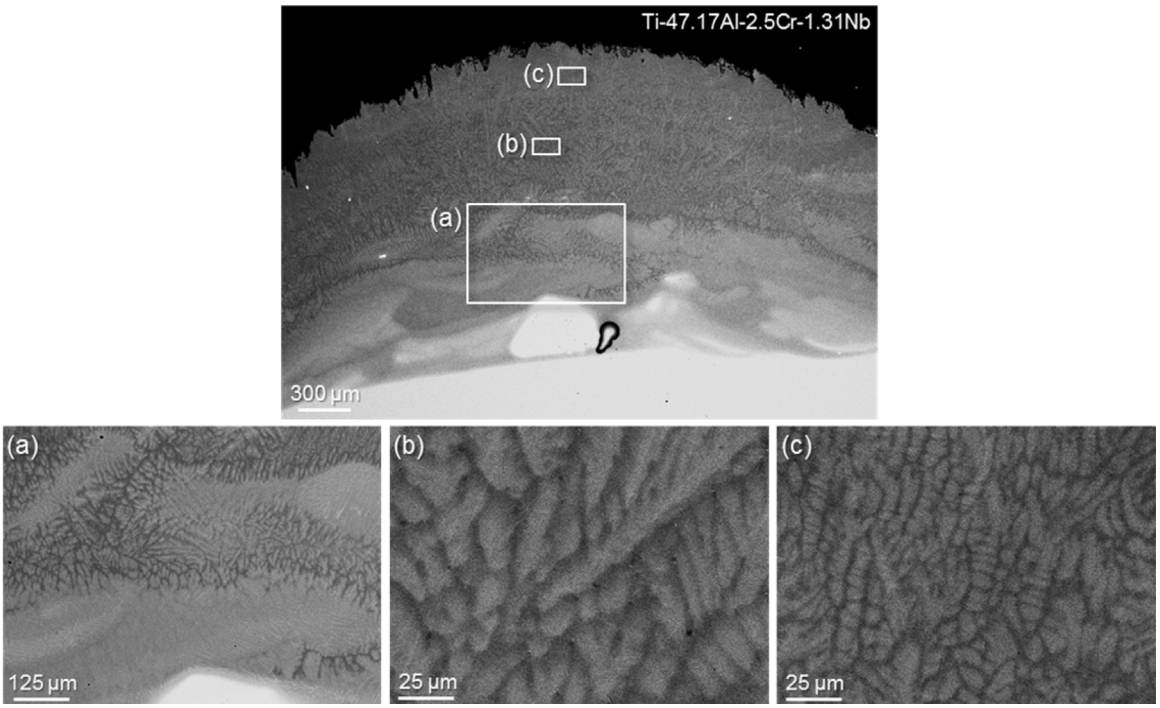

Fig. 14. SEM images of $\alpha_2 + \gamma$ two-phase microstructures with dark TiAl γ phases and light Ti_3Al α_2 phases produced from W + MP with 1400 W, 4.0 $gmin^{-1}$ and composition Ti-46.17Al-2.5Cr-1.31Nb: (a) finer, more equiaxed microstructure due to highest cooling rate; (b) more columnar microstructure; (c) large Ti-rich Ti_3Al α_2-phases due to insufficient mixing with partially-melted Ti wire.

grains within a high-purity Al matrix as shown in Fig. 11. Previous studies have shown that $TiAl_3$ is the first of any titanium aluminide compound to form during reaction synthesis between Ti and Al (Wang et al., 2011), whilst it is the only compound formed in the temperature range 973–1273 K (Sujata et al., 1996). Residual TiO_2 particles can be observed along the Al-rich grain boundary of the dense $TiAl_3$ microstructure, unreacted due to the high oxygen affinity of both Ti and Al.

Large regions of pure Al_2O_3 are also evident in the deposits, primarily at the periphery of each track which can be seen in Fig. 6. Al_2O_3 particulates form as spheres within the dense $TiAl_3$ microstructure, along grain boundaries and within the bulk grain structure. As the Al_2O_3 solidifies while the metallic compounds are still molten, spherical particle reinforcement can be formed. The existence of TiO_2 and Al_2O_3 at the grain boundaries is likely to increase the sensitivity of the deposits to solidification cracking (Mathers, 2002). Columnar TiAl interface grains (~15 μm length) form at the substrate-deposit boundary. The presence of vanadium would suggest that Al has diffused into the substrate to form TiAl as found by Thuillard et al. (1988). However, Luo and Acoff (2004) have indicated that diffusion of Ti towards high Al concentration is dominant, whilst cross-diffusion of both Ti and Al has been reposted by Xu et al. (2006). The plot line EDX chemical composition data in Fig. 12 illustrates this change across the interface.

3.3.2. Combined wire and single powder feedstock

The aim was to achieve the $\alpha_2 + \gamma$ two-phase microstructure that forms around the 50% Al (at%) composition, as seen in the Ti-Al phase diagram. As shown in Fig. 13, a two-phase microstructure is evident within the tracks. EDX indicates that the dark phases are γ-TiAl and the light phases are α_2-Ti_3Al, forming the desired $\alpha_2 + \gamma$ two-phase composition. The two-phase microstructure extends out as dendrites from the Ti dense α_2 section at the centre of the track shown in Fig. 13(c). The dendrites then form a columnar type microstructure mid-way up the track, shown in Fig. 13(b), and finally at the periphery of the track a much finer equiaxed two-phase structure can be seen in Fig. 13(c). This microstructure development seen from the centre to the edge of the tracks follows the rapid cooling rates that occur with the DMD process, where grain growth is in the opposite direction to heat flux. In tracks where the Ti wire has not fully mixed with the powder feedstock, large central regions rich in Ti result in grains developing in the α_2 region to produce Ti_3Al. The obtained microstructure is different to those produced by conventional techniques, which are often formed of lamellar or duplex microstructures as seen in work reviewed by Kothari et al. (2012). Here, the microstructures are akin to those produced by Srivastava et al. (2001) using the DMD process with a Ti-48Al-2Mn-2Nb pre-alloyed powder feedstock.

The tracks produced with a 2.0 $gmin^{-1}$ PFR formed singularly α_2 phase, as expected from Al compositions of ~26-29 at%. The grain structure produced indicates that the melt pool temperature has been raised above the beta-transus line and solidified down into the α_2 region. The grain structure is observed to be more homogenous than the other PFR tracks, and it is believe that this is due to improved mixing from the reduced quantity of material that is being processed. Tracks produced with a 4.8 $gmin^{-1}$ PFR formed exclusively γ phase. The grain structure largely varied across the cross-sections of the tracks from coarse equiaxed to very long columnar grains and considerable amount of cracking was present within the track.

Titanium aluminides with a two-phase $\alpha_2 + \gamma$ microstructure produce mechanical properties that are more aligned with those required for aerospace applications where nickel-based superalloys are used (Kim, 1989). Pure α_2 phase or γ phase microstructures are less suited to such applications due to unsuitable extremes of mechanical properties; particularly issues with ductility. Achieving this two-phase microstructure without the need for pre-alloyed feedstock provides great promise for this combined wire and powder feedstock technique. Despite the lower and higher PFR tracks producing less useful α_2 phase or γ phase microstructures, the ability to successfully alter the composition through manipulation of the processing parameters presents the possibility of functional grading using this technique. Despite issues of mixing in these single tracks, when moving to producing bulk parts the remelting of tracks due to adjacent tracks and layers will help remove the issue and help to ensure the constituent materials are more evenly mixed in-situ.

3.3.3. Combined wire and loose mixed powder feedstock

W + MP tracks processed with the 4.0 $gmin^{-1}$ PFR successfully achieved the $\alpha_2 + \gamma$ two-phase microstructure with the addition of the Cr and Nb additives interspersed throughout. The microstructure from the centre of the track displayed the same characteristics as the Ti-50Al tracks, advancing from dendritic, to columnar, to fine equiaxed from the centre towards the periphery. Fig. 14 depicts this microstructural growth for the W + MP track with 4 $gmin^{-1}$ PFR and 1400 W LP. The similarity between the $\alpha_2 + \gamma$ two-phase microstructure produced in this study and that by Srivastava et al. (2001) with pre-alloyed Ti-48Al-2Mn-2Nb feedstock shows promise for the combined wire and loose mixed powder processing method. It provides greater flexibility over alloying compositions and enables cost and energy savings. The key issue is whether the micro-alloy elements have mixed and dispersed homogenously. The satelliting technique could be used to improve this homogeneity issue, utilising Al powder adhered with micro-alloying elements and replacing the need for loose mixed powder. By using satellited feedstocks for production of Ti-48Al-2Cr-2Nb alloys in this manner and for future titanium aluminides, improvements in the distribution of the micro-alloying elements and the compositional consistency across the track could be made without sacrificing the versatility from using elemental powders.

4. Conclusions

- All three feedstock techniques successfully produce titanium aluminides in-situ with varying success in quality of track deposits, composition, and the microstructures produced.
- Intermetallic matrix composites consisting of a $TiAl_3$ matrix interspersed with Al_2O_3 particulates have been produced at much lower energy densities than through previous processing of other feedstocks, demonstrating the capabilities of in-situ processing.
- The production of the $\alpha_2 + \gamma$ two phase microstructure from simultaneous wire and powder feedstock techniques with a similar grain structure, with the inclusion of micro-alloying elements, to those produced from pre-alloyed feedstocks is very promising. Particularly for utilising this technique as a cheaper and more versatile alternative to pre-alloyed feedstocks and a step to producing functionally graded titanium aluminides.
- The feedstock techniques presented provide alternative methods for producing titanium aluminides with potentially large energy and costs savings over using pre-alloyed feedstocks. The microstructures produced need to be further characterised and the effects of the processing parameters more closely related to be able to more accurately control and tailor them. However, the variety of microstructures and compositions produced provide at least a proof of concept of achieving functionally graded titanium aluminide parts using this technique.
- Based upon quotes from material suppliers LPW Technology Ltd., UK and Goodfellow Cambridge Ltd., UK, the use of constituent Ti, Al, Cr, and Nb powders as used in this study can result in a 40% material cost reduction compared to using pre-alloyed Ti-48Al-2Cr-2Nb. Further costs are saved due to the ability to create alloy variations, recoverability of constituent powders and the elimination of the pre-alloying processing step, further reducing the lifecycle costs of the materials and final components.

Acknowledgements

This work was funded through the EPSRC (Engineering and Physical Sciences Research Council, UK) Centre for Doctoral Training in Additive Manufacturing and 3D Printing (EP/L01534X/1). The authors would also like to thank Mr Stuart Branston for his assistance with operation and running of the laser deposition without whom this work would not be possible.

References

Appel, F., Brossmann, U., Christoph, U., Eggert, S., Janschek, P., Lorenz, U., Müllauer, J., Oehring, M., Paul, J.D., 2000. Recent progress in the development of gamma titanium aluminide alloys. Adv. Eng. Mater. 2, 699–720.

Cárcel, B., Serrano, A., Zambrano, J., Amigó, V., Cárcel, A., 2014. Laser cladding of TiAl intermetallic alloy on ti6Al4V-process optimization and properties. Physics Procedia 56, 284–293.

Dimiduk, D., 1999. Gamma titanium aluminide alloys—an assessment within the competition of aerospace structural materials. Mater. Sci. Eng.: A 263, 281–288.

Fu, P.X., Kang, X.H., Ma, Y.C., Liu, K., Li, D.Z., Li, Y.Y., 2008. Centrifugal casting of TiAl exhaust valves. Intermetallics 16, 130–138.

Imayev, R., Imayev, V., Oehring, M., Appel, F., 2007. Alloy design concepts for refined gamma titanium aluminide based alloys. Intermetallics 15, 451–460.

Kim, Y.-W., 1989. Intermetallic alloys based on gamma titanium aluminide. Jom 41, 24–30.

Kothari, K., Radhakrishnan, R., Wereley, N.M., 2012. Advances in gamma titanium aluminides and their manufacturing techniques. Prog. Aerosp. Sci. 55, 1–16.

Löber, L., Schimansky, F.P., Kühn, U., Pyczak, F., Eckert, J., 2014. Selective laser melting of a beta-solidifying TNM-B1 titanium aluminide alloy. J. Mater. Process. Technol. 214, 1852–1860.

Lasalmonie, A., 2006. Intermetallics: why is it so difficult to introduce them in gas turbine engines? Intermetallics 14, 1123–1129.

Liu, C., Maziasz, P., 1998. Microstructural control and mechanical properties of dual-phase TiAl alloys. Intermetallics 6, 653–661.

Loria, E.A., 2000. Gamma titanium aluminides as prospective structural materials. Intermetallics 8, 1339–1345.

Luo, J.-G., Acoff, V.L., 2004. Using cold roll bonding and annealing to process Ti/Al multi-layered composites from elemental foils. Mater. Sci. Eng.: A 379, 164–172.

Ma, Y., Cuiuri, D., Hoye, N., Li, H., Pan, Z., 2014. Effects of wire feed conditions on in situ alloying and additive layer manufacturing of titanium aluminides using gas tungsten arc welding. J. Mater. Res. 29, 2066–2071.

Mahamood, R.M., Akinlabi, E.T., Shukla, M., Pityana, S., 2012. Functionally graded material: an overview. In: Proceedings of the World Congress on Engineering, WCE 2012.

Mathers, G., 2002. The Welding of Aluminium and Its Alloys. Woodhead publishing.

McElroy, S., Yang, D., Reddy, R., 2000. Laser processing of titanium aluminides. J. Mater. Eng. Perform. 9, 506–515.

Mok, S.H., 2007. Deposition of TI-6Al-4V Using a High Power Diode Laser and Wire, Deposition of TI-6Al-4 V Using a High Power Diode Laser and Wire. The University of Nottingham.

Paul, J., Lorenz, U., Oehring, M., Appel, F., 2013. Up-scaling the size of TiAl components made via ingot metallurgy. Intermetallics 32, 318–328.

Qu, H., Wang, H., 2007. Microstructure and mechanical properties of laser melting deposited γ-TiAl intermetallic alloys. Mater. Sci. Eng.: A 466, 187–194.

Schloffer, M., Iqbal, F., Gabrisch, H., Schwaighofer, E., Schimansky, F.-P., Mayer, S., Stark, A., Lippmann, T., Göken, M., Pyczak, F., 2012. Microstructure development and hardness of a powder metallurgical multi phase γ-TiAl based alloy. Intermetallics 22, 231–240.

Shishkovsky, I., Smurov, I., 2012. Titanium base functional graded coating via 3D laser cladding. Mater. Lett. 73, 32–35.

Shishkovsky, I., Missemer, F., Smurov, I., 2012. Direct metal deposition of functional graded structures in Ti-Al system. Physics Procedia 39, 382–391.

Srivastava, D., Chang, I., Loretto, M., 2001. The effect of process parameters and heat treatment on the microstructure of direct laser fabricated TiAl alloy samples. Intermetallics 9, 1003–1013.

Sujata, M., Bhargava, S., Sangal, S., 1996. Microstructural features of TiAl 3 base compounds formed by reaction synthesis. ISIJ Int. 36, 255–262.

Syed, W.U.H., Pinkerton, A.J., Li, L., 2005. A comparative study of wire feeding and powder feeding in direct diode laser deposition for rapid prototyping. Appl. Surf. Sci. 247, 268–276.

Tetsui, T., Miura, Y., 2002. Heat-resistant cast TiAl alloy for passenger vehicle turbochargers. Mitsubishi Heavy Ind. Tech. Rev. 39.

Thomas, M., Bacos, M., 2011. Processing and characterization of tiAl-based alloys: towards an industrial scale. J. Aerosp. Lab, 1–11.

Thuillard, M., Tran, L., Nicolet, M.-A., 1988. Al_3Ti formation by diffusion of aluminum through titanium. Thin Solid Films 166, 21–28.

Wang, Y., Wang, J., Xia, Q., Yang, J., 2000. Microstructure refinement of a TiAl alloy by beat treatment. Mater. Sci. Eng. A 293, 102–106.

Wang, P.-y., Li, H.-j., Qi, L.-h., Zeng, X.-h., Zuo, H.-s., 2011. Synthesis of Al-TiAl3 compound by reactive deposition of molten Al droplets and Ti powders. Prog. Nat. Sci.: Mater. Int. 21, 153–158.

Xu, L., Cui, Y., Hao, Y., Yang, R., 2006. Growth of intermetallic layer in multi-laminated Ti/Al diffusion couples. Mater. Sci. Eng.: A 435, 638–647.

Zhang, X., Brice, C., Grylls, R., Evans, D., Fraser, H., 1998. Characterization of Laser-Deposited TiAl Alloys, MRS Proceedings. Cambridge Univ Press (p. KK5. 2.1).

Zollinger, J., Lapin, J., Daloz, D., Combeau, H., 2007. Influence of oxygen on solidification behaviour of cast TiAl-based alloys. Intermetallics 15, 1343–1350.